

Stimulation of Insulin Signaling and Inhibition of JNK-AP1 Activation Protect Cells from Amyloid- β -Induced Signaling Dysregulation and Inflammatory Response

Michelle Bamji-Mirza^{a,b}, Debbie Callaghan^a, Dema Najem^{a,b}, Shanshan Shen^{a,c},
Mohamed Shaad Hasim^{a,b}, Ze Yang^d and Wandong Zhang^{a,b,c,*}

^aHuman Health Therapeutics Portfolio, National Research Council Canada, Ottawa, ON, Canada

^bFaculty of Medicine, University of Ottawa, Ottawa, ON, Canada

^cSoutheast University, Nanjing, China

^dBeijing Hospital & Beijing Institute of Geriatrics, Chinese Ministry of Health, Beijing, China

Accepted 30 October 2013

Abstract. One of the hallmarks of Alzheimer's disease (AD) is the accumulation and deposition of amyloid- β (A β) peptides in the brain and cerebral vasculature. A β evokes neuroinflammation and has been implicated in insulin signaling disruption and JNK-AP1 activation, contributing to AD neuropathologies including oxidative injury and vascular insufficiencies. In this study we aim to better understand the protective mechanisms of insulin signaling and JNK-AP1 inhibition on the adverse effects of A β . Four-hour treatment of hCMEC/D3, the immortalized human brain endothelial cells (iHBEC), with A β ₁₋₄₂ resulted in significant c-Jun phosphorylation, oxidative stress, and cell toxicity. Concurrent treatment with A β ₁₋₄₂ and insulin or A β ₁₋₄₂ and JNK inhibitor SP600125 significantly improved cell viability. Cytokine array on conditioned media showed that insulin and SP600125 strongly reduced all A β ₁₋₄₂-induced cytokines. ELISA confirmed the protective effect of insulin and SP600125 on A β -induced expression of interleukin (IL)-8 and Growth related oncogene- α (Gro- α). qRT-PCR revealed that insulin and SP600125 protected iHBEC from A β ₁₋₄₂-induced inflammatory gene expression. Transcription factor profiling showed that treatment of iHBEC with A β ₁₋₄₂, insulin, or SP600125 alone or in combination resulted in profound changes in modulating the activities of multiple transcription factors and relevant pathways, some of which were validated by western blot. Insulin treatment and JNK inhibition *in vitro* synergistically reduced c-Jun phosphorylation and thus JNK-AP1 signaling activation. The study suggests that activation of insulin and blocking of JNK-AP1 signaling inhibits A β -induced dysregulation of insulin signaling and inflammatory response.

Keywords: Alzheimer's disease, amyloid- β peptides, inflammatory response insulin signaling, JNK-AP1 signaling

INTRODUCTION

AD and type II diabetes mellitus (T2DM) are increasing at an alarming rate and are major health con-

cerns for society. Individuals with T2DM have a greater risk of developing AD and vascular dementia [1]. The prevailing "amyloid cascade" hypothesis in AD proposes that the accumulation and oligomerization of A β peptides leads to neurotoxicity and neuroinflammation [2]. The amyloid cascade hypothesis alone fails to explain all of the histopathological, molecular, and biochemical abnormalities occurring in AD brain.

*Correspondence to: Dr. Wandong Zhang, National Research Council Canada, 1200 Montreal Road, Building M-54, Ottawa, ON, K1A 0R6, Canada. Tel.: +1 613 993 5988; Fax: +1 613 941 4475; E-mail: Wandong.Zhang@nrc.ca.

Insulin exerts numerous actions on the brain, including glucose regulation, neuronal growth/survival, memory, synaptic plasticity, and cerebral vasoreactivity. Insulin deficiency or an “insulin-resistant brain state” mechanistically interlinks all of the neuropathologies prevalent in AD [3].

T2DM and AD share some common cellular and molecular mechanisms. AD brain tissue has shown to exhibit elevated levels of IRS-1pSer and activated JNK, analogous to peripheral tissues in patients with T2DM [4]. Impaired IRS-1 signaling was observed in rat cultured hippocampal neurons and brains of cynomolgus monkeys treated with A β [4], and in hippocampi of Tg-AD mice [4, 5]. In AD brain, impaired insulin signaling results in decreased phosphoinositide-kinase (PI3-K)/Akt activity and increased glycogen synthase kinase (GSK)3 β activity leading to increased tau hyperphosphorylation, a pathological feature of AD neurofibrillary tangles [6]. Short term exposure of A β to cerebral synaptosomes from Sprague-Dawley rats resulted in lipid peroxidation and a significant decrease in glucose transport [7] suggesting that impairments in insulin signaling and glucose utilization occur during the early stages of AD, prior to significant A β plaque burden. A β has been shown to competitively bind the insulin receptor (IR), and reduce insulin binding and receptor autophosphorylation of the IR in human placental plasma membranes (used as a rich source of human insulin receptors) [8]. A β peptide affects insulin levels through competitive binding of the insulin degrading enzyme, an enzyme involved in the degradation of both insulin and A β peptides [9]. Reduced insulin degrading enzyme protein levels and activity also occur in AD brain [10]. A β peptides can be transported across cerebral microvessels and capillaries and deposited in the vessels, resulting in cerebral amyloid angiopathy [11]. Impairments in cerebrovascular integrity leading to disruption of the blood-brain barrier and resulting in vascular insufficiencies, inflammation, and oxidative stress, occur via a RAGE receptor-mediated process in both T2DM and AD [11, 12].

Therapies against AD have focused on targeting A β peptides; either to dissolve plaques or to inhibit A β peptide aggregation, with only moderate success. Targeting A β peptides alone will be insufficient to address the pleiotrophic causes of AD neuropathology. New therapies against AD must consider the impact of dysregulation of insulin signaling in AD pathology, and target the factors that will alleviate insulin resistance and restore normal insulin signaling events. C-Jun N-terminal kinase (JNK) is one of the key

proteins involved in insulin resistance; inhibitory serine phosphorylation of IRS-1 by JNK creates a negative feedback mechanism to down regulate insulin signaling [13, 14]. Our previous work demonstrated that A β peptides can activate JNK-AP1 signaling pathway and upregulate the expression of inflammatory genes in iHBEC (hCMEC/D3) [15], leading us to postulate that enhancing insulin signaling and suppressing JNK activity may inhibit these A β -induced effects. Our previous and others' studies have shown that a JNK inhibitor SP600125 can inhibit A β -induced JNK-AP1 signaling and the expression of inflammatory genes in HBEC [15–17]. JNK activation is also involved in neuroinflammation and neurovascular inflammation induced by hypoxia/ischemia or inflammatory factors [18–20]. Since HBEC are involved in A β transport across the blood-brain barrier and neurovascular inflammation in AD [15, 21] and diabetes results in cerebrovascular complications and contributes to the development of vascular dementia and AD [22], we believe that insulin signaling and JNK-AP1 signaling may cross-react with each other in AD neurovascular inflammation as a result of aberrant A β transport and deposition on HBEC. In the present study, we show that A β -induced toxicity and inflammatory response in iHBEC can be reduced with insulin and the JNK inhibitor SP600125. We identify multiple cytokines and transcription factors (TFs) changing in response to treatment with A β , insulin, and SP600125 in iHBEC, highlighting shared and divergent pathways between insulin and A β . Synergistic effects were also achieved with the combination of insulin and SP600125 on A β -treated cells.

MATERIALS AND METHODS

Materials

iHBEC base media EBM-2 (#cc-3156) was purchased from Lonza (Walkersville, MD, USA). Fetal bovine serum (FBS) was purchased from Hyclone (Logan, UT, USA). Penicillin-streptomycin (#P0781), Hepes (#H4034), basic fibroblast growth factor (bFGF) (#F0291), recombinant human insulin (#91077C), and protease inhibitor cocktail (#P8340) were purchased from Sigma Aldrich Canada Ltd. (Oakville, Ontario, Canada). Trypsin/EDTA without Ca²⁺/Mg²⁺ (#25200-056), human IL-8 ELISA kit (#KHC0081), MTT (#M6494) and TRIzol (#15596-018) were purchased from Life Technologies (Burlington, Ontario, Canada). The BSA standard (#500-0007), DCTM

protein assay kit (#500-0112), Experion RNA Std-Sens analysis kit (#700-7153), SsoFast EvaGreen Supermix (#172-503), iScript cDNA synthesis kit (#170-8891), and PVDF membrane (#162-0177) were purchased from Bio-Rad (Hercules, CA, USA). The 1 \times RIPA buffer (#9806) and phospho-Rb (Ser807/811) (#8516P), Rb (4H1) (#9309P), phospho-I κ B α (Ser32) (14D4) (#2859P) and I κ B α (44D4) (#4812S) antibodies were purchased from Cell Signaling Technology Inc. (Boston, MA, USA). Ambion DNA-freeTM Kit (#AM1906) was purchased from Applied Biosystems Inc. (Carlsbad, CA, USA). Trichloroacetic Acid (TCA #A322-500) and Bio-dyne B Nylon 0.45 μ m membrane (#77016) were purchased from Fisher Scientific Inc. (Ottawa, ON, Canada). The SP600125 JNK inhibitor (#S7979) was purchased from LC Laboratories (Woburn, MA, USA). Recombinant A β ₁₋₄₂ (#A-1166-1) and A β _{1-42scrambled} peptides (#A-1004-1) were purchased from r-Peptides (Bogart, Georgia, USA). Combo Protein/DNA transcription factor arrays (#MA1215), Nuclear Extraction kit (#AY2002) were purchased from Affymetrix, Inc. (Santa Clara, CA, USA). Phospho-c-Jun (Ser63 #9261, Ser73 #9164), phospho-IGF-1 receptor b (tyr 1135/1136)/insulin receptor b (Tyr 1150/1151) (19H7) rabbit mAb #3024 specific antibodies were purchased from New England Biolabs (Pickering, Ontario, Canada). Western-Lighting Plus-ECL (#NEL105001EA) was purchased from Perkin Elmer Inc. (Waltham, Massachusetts, USA). Autoradiography film (#MSF-BX810) was purchased from Mandel Scientific (Guelph, Ontario, Canada). OxiSelectTM HNE-His Adduct ELISA Kit was purchased from Cell Biolabs, Inc. (San Diego, CA, USA). Human (#ARY005) cytokine Arrays and Gro- α human ELISA kit (#DRG00) were purchased from R&D Systems (Minneapolis, MN, USA). geNorm human reference gene primer kit and Biogazelle qbase analysis software were purchased from PrimerDesign Ltd. (Rownhams, Southampton, United Kingdom). Hank's balanced salt solution (HBSS cat #311-513CL) was purchased from Wisent (Montreal, Quebec, Canada). All qPCR primers and EMSA oligonucleotides were purchased from Integrated DNA Technologies (IDT, Coralville, Iowa, USA).

iHBEC cell culture and treatments

hCMEC/D3 cells (iHBEC) were obtained from the laboratory of Dr. P-O Couraud (Paris, France), and are well characterized [23]. The cells were plated on rat tail collagen type 1 (100 μ g/mL)-coated tissue

culture dishes and maintained in EBM-2 media containing 5% FBS, 1% penicillin-streptomycin, 10 mM Hepes, and 1 ng/mL basic human fibroblast growth factor at 37°C and 5% CO₂. iHBEC were passaged using trypsin/EDTA without Ca²⁺/Mg²⁺. Unless otherwise stated, confluent (90–95%) dishes were treated for various treatment times with 10 μ M A β ₁₋₄₂ or A β _{1-42scrambled} peptide (prepared in 0.25% acetic acid), 1.7 μ M human insulin (prepared in H₂O, adjusted to pH 3), or 25 μ M SP600125 (prepared in dimethyl sulfoxide) alone or in combination with A β ₁₋₄₂ or A β _{1-42scrambled} peptide.

Immunoblot analysis

After treatment, iHBEC were washed 2 times with HBSS and lysed in sample buffer [5% glycerol, 5% β -mercaptoethanol, 3% sodium dodecyl sulphate (SDS), 0.05% bromophenol blue, and 10 mM Tris-HCl, pH 6.8] or in RIPA buffer supplemented with 1% Triton X-100 and sonicated 2 \times 20 s in a water bath sonicator. The cell lysates were boiled at 100°C for 10 min, centrifuged at 15,000 rpm for 10 min at 4°C, and the clarified supernatants were stored at –80°C until use. The protein concentration of each sample was determined by TCA assay or by DC assay system (BioRad) following manufacturers' instructions. TCA was carried out in clear 96-well plates (Costar) by combining sample, sample buffer and water (100 μ L) with 60% trichloroacetic acid prepared in water (66.7 μ L) and incubating at 37°C for 15 min to precipitate the proteins. A reference standard curve was obtained using BSA prepared in sample buffer. Turbidity measurements of samples or BSA standards were measured at 570 nm. Protein concentration of each sample was calculated relative to the BSA standard curve and reported in μ g/ μ L. Proteins were resolved on a 10% SDS polyacrylamide gel at 125 V in running buffer (25 mM Tris, 192 mM glycine, and 0.35 mM SDS), and transferred to PVDF membrane at 150 mAmps overnight in transfer buffer (25 mM Tris, 192 mM glycine, and 20% methanol). Proteins were detected by overnight incubation with a 1 : 1000 dilution of their respective primary antibodies in 1% milk in Tris buffered saline with 0.05% Tween-20 buffer (TBST, 10 mM Tris, pH 8.0, 150 mM NaCl, 0.05% Tween-20, and 1% skim milk powder), next a 1 h incubation with a 1 : 3000 dilution of IgG-HRP secondary antibody in 5% milk TBST, followed by incubation with ECL Plus reagent and visualization on autoradiography film. Densitometry values were determined using Un-Scan-It software (Silk Scientific Inc.).

HNE oxidative stress assay

The HNE-His Adduct ELISA kit was used to determine the levels of 4-hydroxy-2-trans-nonenal (HNE), a natural byproduct of lipid oxidation, following the manufacturer's instructions. Briefly, the treated iHBEC were washed twice with HBSS and scraped in PBS supplemented with protease inhibitors. The samples were lysed in a water bath sonicator, centrifuged at 14,000 rpm for 15 min at 4°C, and the clarified supernatants were stored at -80°C until future use. Protein concentration was determined by DC assay system (BioRad). The samples were diluted with PBS to 10 μ g/mL, added to the ELISA plate, and incubated overnight at 4°C. HNE-protein adducts in the sample or HNE-BSA standard were probed with anti-HNE-His antibody for 1 h followed by HRP-conjugated secondary antibody (for 1 h). Absorbance of each well was read at 450 nm using a Spectra Max 340 spectrophotometer (Molecular Devices, Sunnyvale, CA). The sample HNE adduct amount was determined with reference to the HNE-BSA standard curve, and the data were presented as fold-change of A β ₁₋₄₂-treated against A β _{scrambled} (A β _{sc})-treated cells.

MTT assay

iHBEC were plated in 96-well format and grown to 75% confluency. The cells were treated for 24, 48, or 72 h. Post treatment, the media were replaced with 100 μ L of fresh media containing 0.45 mg/mL MTT reagent [3-(4,5-dimethylthiazolyl)-2,5-diphenyltetrazolium bromide]. The cells were incubated for 1 h in at 37°C and 5% CO₂ to allow for formation of formazan crystals. The formazan crystals were dissolved by addition of 10% SDS/0.01 N HCl (100 μ L) during a 4-h incubation at 37°C and 5% CO₂. Colorimetric change was measured on a spectrophotometer at an absorbance of 570 nm. Data was expressed as percent viability relative to vehicle.

Cytokine array

Human Cytokine Proteome Profiler™ Array was used to determine the changes in secreted cytokines from 4-h treated iHBEC following manufacturer's instructions. Briefly, media were collected from treated iHBEC, centrifuged at 200 \times g for 5 min, and the clarified media were stored at -80°C for future use. The experiment was repeated three times for each

treatment group ($n=3$). To ensure each experimental repeat was represented equally on each array, equal volumes of media from each independent treatment ($n=1, 2, \text{ and } 3$) were pooled. One membrane array was prepared for each of the following treatment groups, 10 μ M A β _{1-42sc} peptide, 10 μ M A β ₁₋₄₂, 1.7 μ M insulin, 25 μ M SP600125, 10 μ M A β ₁₋₄₂ in combination with 1.7 μ M insulin, 10 μ M A β _{1-42sc} peptide in combination with 1.7 μ M insulin, 25 μ M SP600125 in combination with 10 μ M A β ₁₋₄₂, and 25 μ M SP600125 in combination with 10 μ M A β _{1-42sc} peptide. The media samples (pooled $n=3$) were mixed with a cocktail of cytokine-selective biotinylated antibodies. The sample/antibody mix was then incubated with its representative array overnight at 4°C with gentle shaking to allow for capture to cognate immobilized antibodies present on each membrane. Visualization of cytokines was achieved with streptavidin-HRP and chemiluminescent detection exposed to film. Densitometry of each spot was determined using Un-Scan-it software, and the results were presented as fold-change relative to A β _{1-42sc} peptide control. Significant changes were set at >1.25-fold change relative to A β _{sc}, as per manufacturers' instructions. The Database for Annotation, Visualization and Integrated Discovery (DAVID) version 6.7 was used for functional annotation clustering of identified cytokines (<http://david.abcc.ncifcrf.gov/>) [24].

ELISA

The media from the 4-h treated iHBEC were collected and spun at 200 \times g for 5 min, and the clarified media were stored at -80°C until use. The cells in each well were fixed with 4% formalin and counted using Countess Automated Cell Counter (Invitrogen), and this was used to normalize the data. The levels of secreted IL-8 protein were measured with a commercial ELISA kit as per the manufacturer's instructions. Briefly, the media were diluted between 2–6 times with the dilution buffer and 50 μ L of each diluted sample was added to the ELISA plate. The concentration of IL-8 in the samples was determined by comparing the absorbance of the samples to the standard curve, and data were presented as pg IL-8/mL/ 1×10^5 cells. To determine the secreted levels of Gro- α from treated iHBEC, the media were retrieved and processed as described above for IL-8 ELISA and a human CXCL1/Gro- α immunoassay ELISA kit was used. Gro- α cytokine levels were presented in pg Gro- α /mL.

Table 1
Primers for real-time RT-qPCR

Gene	Sense primer (5'-3')	Anti-sense primer (5'-3')	Program
Actin	TGTCCACCTTCCAGCAGATGT	AGTCCGCCTAGAAGCATTTGC	2-Step Amp+Melt Tm 55
IL-8	AGCTGGCCGTGGCTCTCT	TTAGCACTCCTTGGCAAACTG	2-Step Amp+Melt Tm 55
Gro- α	AGCCTGCAACATGCCAGCCAC	TGTGCACATACATCCCCTGCCTTC	2-Step Amp+Melt Tm 55
IL-32- α	CGTGGGGCTCCGTAGGACTTGT	GTAGCTGCCTTCTGCTCTCCAGCG	3-Step Amp+Melt Tm 52
GM-CSF	CATGATGGCCAGCCACTACAA	ACTGGCTCCCAGCAGTCAAAG	3-Step Amp+Melt Tm 55
MIP-1 β	GTAGCTGCCTTCTGCTCTCCAGCG	CGCAGTGTAAGAAAAGCAGCAGGCG	3-Step Amp+Melt Tm 55
TNF- α	CTCTGGCCAGGCAGTCAGATCA	CGGCGTTCAGCCACTGGAG	3-Step Amp+Melt Tm 55
IL-23- α	CAGGGGAGCCTTCTCTGCTCC	ACCCTCAGGCTGCAGGAGTTG	3-Step Amp+Melt Tm 52
IL-2	GCACTTGTCAAAACAGTGCACCTA	TGTGAGCATCCTGGTGAGTTTGGG	3-Step Amp+Melt Tm 52

RNA isolation and qPCR

Total RNA was extracted from 4-h treated iHBEC using TRIzol reagent, DNA contaminants were removed using Ambion DNA-free clean-up kit, and RNA quality and integrity were confirmed using Experion Automated Electrophoresis Station and Experion RNA StdSens analysis kit following appropriate manufacturer's instructions. RNA concentration was measured with NanoDrop 1000 UV-Vis spectrophotometer, and 1 μ g of total RNA was reverse-transcribed using iScriptTM cDNA synthesis to a volume of 20 μ l according to manufacturer's instructions. qPCR analysis was performed using specific primers designed against Genbank sequences and Primer-Blast (<http://www.ncbi.nlm.nih.gov/tools/primer-blast/>) programs. Primers were then synthesized by IDT Technologies as listed in Table 1. The reactions were carried out using SsoFast EvaGreen supermix in a final volume of 20 μ L using 2-stepAmp+melt program with the conditions 95°C/3:00, 95°C/0:10, 55°C/0:30, go to step 2 39x, 95°C/0:10, 65°C/0:05, 95°C/0:50 or 3-stepAmp+melt program 95°C/3:00, 95°C/0:10, 55°C/0:10, 72°C/0:30 go to step 2 39x, 95°C/0:10, 65°C/0:05, 95°C/0:50 in a CFX96TM real-time PCR detection system instrument. A no-template control was performed for each primer pair to test buffers, solutions and cDNA preparations for contamination and to test for the possibility of primer-dimers. The PCR efficiency was assessed by performing standard curves using pooled cDNA material by plotting the log of the starting quantity of the template against the Cq values to determine the equation of the linear regression line. To choose the appropriate reference gene, geNorm reference gene primer kit was purchased and the samples were tested and analyzed using Biogazelle.com qBasePlus software. Relative quantification of each target gene was normalized against β -actin housekeeping gene. Fold-

change for each gene was calculated using relative quantification where average control/vehicle values were set to 1. Gene expression levels were expressed as relative abundance \pm SEM.

Transcription factor array

iHBEC were treated with A β ₁₋₄₂ (10 μ M), A β _{sc} peptide (10 μ M), insulin (1.7 μ M), and SP600125 (25 μ M) alone or in combination with A β peptides for 4 h. Nuclear isolations were prepared following manufacturer's instructions for each treatment group in three separate experiments and pooled for array application. To ensure each experimental repeat was represented equally on the TF array, equal amounts of nuclear lysate from each independent treatment ($n = 3$) were pooled. Each of the pooled samples, representing a treatment group (totaling 7.5 μ g of nuclear material), was incubated with biotin-labeled DNA-binding oligonucleotides to form protein/DNA complexes. The protein/DNA complexes were separated from the free biotin-labeled DNA oligonucleotides by spin columns. The probes from the protein/DNA complexes were then extracted and hybridized onto independent arrays overnight at 42°C in a rotating hybridization oven. TF changes were visualized using a chemiluminescence detection system and exposed to film. Densitometry values of each spot were determined using Un-Scan-it software and results were presented as fold-change relative to A β _{1-42sc} peptide control. Significant changes were set at >2-fold change relative to A β _{sc}, as per manufacturers' instructions. TF changes for each treatment were classified into three groups, namely shared pathways, divergent pathways and independent pathways in terms of A β ₁₋₄₂ and insulin. Of note, brackets preceding the TF name refer to different target sequences within the respective TF. For the list of the TFs examined in this array, please refer to the Supplementary Table 1.

Statistical analysis

All results were reported as mean \pm SEM. Statistical significance was analyzed by unpaired two-tailed *t*-test, for two group comparisons, or by one-way ANOVA, with Bonferroni *post-hoc* tests, for multiple group comparisons, using Prism graphing software. Statistical significance was defined as $p < 0.05$.

RESULTS

Insulin and A β_{1-42} peptides induce signaling events and cellular responses in iHBEC

To validate our *in vitro* iHBEC model system for A β_{1-42} - and insulin-induced signaling pathways, protein phosphorylation analysis by immunoblot and lipid oxidation analysis by quantification of HNE adduct levels were performed. C-Jun is a member of the AP-1 dimeric complex [25] which is phosphorylated by JNK in A β -induced inflammatory events [15]. To examine if c-Jun phosphorylation occur in iHBEC upon A β stimulation, A β_{1-42} peptide (10 μ M) was added to cells for up to 24 h and the protein phosphorylation levels at position serine 63 (ser63) of c-Jun were analyzed by immunoblot. cJun63-phosphorylation levels were increased with A β_{1-42} treatment as compared to A β_{sc} peptide control as early as 1 h post-treatment and remained increased relative to control at each time point examined (Fig. 1A, panel I). Densitometry analysis from three separate experiments and actin normalization showed a significant increase of phosphorylation for c-Jun ser 63 at 4 h (Fig. 1A, panel II, one-way ANOVA, Bonferroni's *post-hoc* test, $*p < 0.05$). Of note, we used a mixed monomeric, oligomeric, and fibril A β_{1-42} preparation as shown (Fig. 1B). The c-Jun ser63 data expands on our previous findings of inflammatory events observed by A β_{1-40} induction by showing that A β_{1-42} peptides also phosphorylate c-Jun ser63 in iHBEC [15]. Activation of JNK signaling by A β peptides represents an inhibition or negative feedback on insulin signaling pathways [4, 13, 26].

To establish if iHBEC were responsive to exogenous insulin stimulation, the cells were treated with 1.7 μ M of insulin for various time points from 10 min to 24 h. Phosphorylation of the IR kinase domain at critical tyrosine residues was increased 10-min, 20-min, 40-min, 1-h, and 4-h post-treatment (Fig. 1C). Densitometry analysis from three separate experiments was averaged, normalized to actin, and demonstrated

that each of these time points was statistically significant (Fig. 1C, one-way ANOVA, Bonferroni's *post-hoc* test $**p < 0.01$ or $*p < 0.05$). Insulin signaling was also analyzed in iHBEC treated with A β_{1-42} (or A β_{sc}), insulin, or JNK inhibitor SP600125 alone or in combination by immunoblot analysis of phospho-IR and phospho-AKT after 20 min of treatment (Supplementary Figure 1B and C, one-way ANOVA, Bonferroni's *post-hoc* test, $*p < 0.05$, $**p < 0.01$, $***p < 0.001$).

Increased oxidative stress is an important factor in the pathology of AD; this includes lipid oxidation of key cellular regulatory proteins [27]. To determine if A β treatment would lead to lipid oxidation in our iHBEC model, we measured HNE-adducts. The cells were treated with A β_{1-42} (10 μ M) for up to 24 h. HNE-adducts were significantly increased at 8 h post-treatment compared to A β_{sc} peptide control (Fig. 1D, one-way ANOVA, Bonferroni's *post-hoc* test, $**p < 0.01$). Together, the increases in c-Jun ser63 phosphorylation, p-IR, and oxidative stress demonstrate that the iHBEC was highly responsive to A β_{1-42} peptide stimulation and exogenous insulin.

During validation of our model system we found that A β_{1-42} induced a significant increase of c-Jun phosphorylation and increased lipid oxidation at 10 μ M, and insulin induced significant phosphorylation of the IR kinase domain at 1.7 μ M. Although both of these concentrations are above physiological levels, these adaptations were appropriate for our model system. We used an immortalized cell line, not a primary cell line, in which cell growth requires both serum and bFGF, which has been shown to be neuroprotective [28–30]. Moreover, we chose A β_{1-42} peptides because a stronger A β stimulus [31] was needed to evoke an inflammatory response in these cells, and A β_{1-42} may play a greater role in the development of cerebral amyloid pathology than previously thought [32] in addition to A β_{1-40} deposits that are mainly found in the vasculature [33, 34]. We and others have found that these supraphysiological concentrations of A β_{1-42} (10 μ M) are necessary to initiate the inflammatory response in this immortalized cell line [35, 36]. Thus, supraphysiological doses are required to activate the signaling pathways of interest for our studies with this immortalized cell *in vitro* model.

Insulin and JNK inhibitor SP600125 protect iHBEC from A β_{1-42} toxicity

It was next determined whether A β treatment would induce toxicity in our cell model system. MTT assay was used to evaluate cell stress. Metabolically active

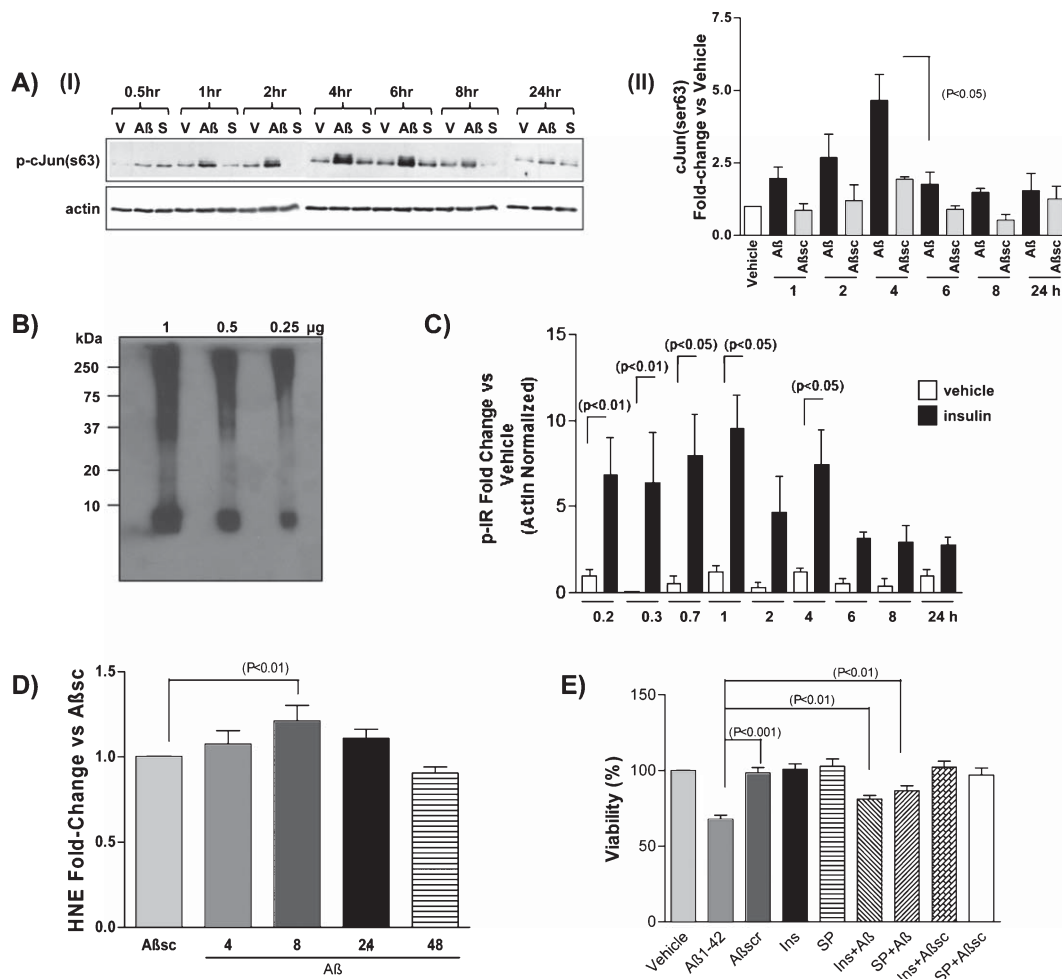


Fig. 1. Insulin and A β ₁₋₄₂ exert cellular changes in iHBECs, and insulin and SP600125 can protect iHBEC from A β ₁₋₄₂-mediated toxicity. A) A β ₁₋₄₂ treatment stimulates c-Jun ser63 phosphorylation in iHBEC. Cells were treated with A β ₁₋₄₂ or A β_{sc} peptides for up to 24 h. Cell-proteins were resolved by SDS-PAGE, transferred to PVDF membrane, and immunoblotted for c-Jun ser63 phosphorylation (A, panel I). The bands were semi-quantified by densitometry analysis and normalized to actin. The data from three separate experiments were averaged and presented relative to vehicle control for c-Jun ser 63 (A, panel II, One-way ANOVA, Bonferroni *post-hoc* test, $*p < 0.05$). V, A β , and S refer to vehicle, A β ₁₋₄₂, and A β_{sc} , respectively. B) Preparation comprised of oligomeric A β ₁₋₄₂. 1, 0.5, and 0.25 μ g of the A β preparation was run on an SDS-PAGE gel and immunoblot was performed using anti-A β antibody. C) Insulin treatment activates insulin signaling pathway in iHBEC. Cells were treated with 1.7 μ M of insulin for up to 24 h, and then cell-proteins were resolved by SDS-PAGE, transferred to PVDF membrane, and immunoblotted for p-IR. Bands were quantified, and data from three separate experiments were averaged, normalized to actin, and presented relative to vehicle (H₂O, pH 3.0) (One-Way ANOVA, Bonferroni's *post hoc* test $**p < 0.01$, $*p < 0.05$). D) A β ₁₋₄₂ treatment causes lipid oxidation in iHBEC. iHBEC were treated with A β ₁₋₄₂ or A β_{sc} peptide control for up to 48 h. Cell supernatants were assayed by ELISA to measure HNE adduct levels. The data from three separate experiments were averaged and presented relative to A β_{sc} peptide control (One-way ANOVA, Bonferroni's *post hoc* test, $**p < 0.01$). E) Insulin and SP600125 can protect iHBEC from A β ₁₋₄₂-mediated toxicity. Cells were treated with A β ₁₋₄₂ (10 μ M) alone or in the presence of either insulin (1.7 μ M) or SP600125 (25 μ M). After 4 h, SP600125 was removed and A β and insulin treatment were continued for a total of 48 h. A second supplement of insulin was added after the first 24 h. Cell toxicity was measured by MTT assay at 48 h post-treatment. The data from three separate experiments were averaged and presented as viability relative to vehicle control ($**p < 0.01$, $*p < 0.05$, One-way ANOVA, Bonferroni's *post-hoc* test).

cells reduce MTT to formazan purple, a colorimetric change which is detected at an absorbance of 570 nm. A β ₁₋₄₂ peptide (10 μ M) induced significant toxicity in iHBEC at all time-points examined (24, 48, and 72 h) (data not shown). To examine if activation of insulin

signaling or inhibition of JNK signaling could protect iHBEC from A β ₁₋₄₂-mediated toxicity, cells were treated with insulin or the JNK inhibitor SP600125 (Fig. 1E). Interestingly, addition of SP600125, only during the first 4 h of A β ₁₋₄₂ addition, was sufficient

Table 2

Functional annotation clustering of identified cytokines using the DAVID database. The official gene symbol of each cytokine that was altered by A β ₁₋₄₂ treatment (Fig. 2A) was entered into the DAVID resource. The annotation chart organized the cytokines into various functional clusters

DAVID annotation cluster	Associated cytokines	p-value
Cytokines and inflammatory response	GM-CSF, IL-6, IL-8	9.30E-04
Cytokine-cytokine receptor interaction	I-309, MIP-1 β , GRO- α , GM-CSF, IL-23, IL-6, IL-8	1.80E-08
Chemokine signaling pathway	I-309, MIP-1 β , GRO- α , IL-8	9.00E-04
Jak-STAT signaling pathway	GM-CSF, IL-23, IL-6	1.30E-02
Regulation of hematopoiesis by cytokines	GM-CSF, IL-6, IL-8	3.00E-04
Erythrocyte differentiation pathway	GM-CSF, IL-6	2.70E-02
Toll-like receptor signaling pathway	MIP-1 β , IL-6, IL-8	5.60E-03
NOD-like receptor signaling pathway	GRO- α , IL-6, IL-8	2.10E-03
Selective expression of chemokine receptors during T-cell polarization	GM-CSF, MIP-1 β	5.10E-02
Cytosolic DNA-sensing pathway	MIP-1 β , IL-6	6.30E-02

IL-32 and TNF- α were not included by DAVID in the annotation.

to reduce A β -induced toxicity when measured after 48 h, suggesting that critical signaling pathways are affected within the first four hours of A β addition. Addition of insulin during the initial treatment ($T=0$) followed by a second supplemental dose at 24 h increased cell viability significantly when measured at 48 h (Fig. 1E, one-way ANOVA, Bonferroni's *post-hoc* test $**p < 0.01$). A one-time dose of insulin at the beginning of treatment ($T=0$) with A β was not sufficient to protect against toxicity when measured at 48 h (data not shown). These data suggest that activation of insulin signaling and inhibition of JNK signaling protect the iHBEC from A β -mediated cellular toxicity.

Insulin and JNK inhibitor protect iHBEC from A β -induced cytokine secretion

We wanted to determine if the observed increases in A β -mediated cell toxicity and the protection offered by activation of insulin signaling, and inhibition of JNK signaling, involved changes in the inflammatory response. The cells were treated for 4 h with A β _{sc} peptide, A β ₁₋₄₂, insulin, and SP600125 alone or in combination with A β , and the protein levels of multiple secreted cytokines from pooled treatment conditions of three independent experiments were determined using the Human Cytokine Proteome ProfilerTM Array. Immunoblot arrays were generated for each treatment and the spots were semi-quantified by densitometry analysis and presented relative to A β _{sc} (Fig. 2A). A β ₁₋₄₂ treatment significantly (which was set at >1.25-fold change relative to A β _{sc}, as per manufacturers' instructions) increased the secreted level of nine cytokines, namely IL-6, IL-8, I-309, MIP-1 β , IL-23, IL-32- α , TNF- α , Gro- α , and GM-CSF, relative to A β _{sc} peptide control (Fig. 2A). The various functions of these cytokines are shown as per DAVID Bioinformatics Resource version 6.7 (Table 2). We

had previously shown that A β ₁₋₄₀ could increase the cytokines IL-6, IL-8, MCP-1, and Gro- α [15]. Here, we show that these cytokines are also increased by A β ₁₋₄₂ peptides along with an additional five cytokines. Six of the nine cytokines that were increased by A β ₁₋₄₂ treatment were significantly reduced with the addition of insulin or SP600125 in combination with A β ₁₋₄₂ relative to A β ₁₋₄₂ alone, namely I-309 (49.8%, 56.8%, panel III), MIP-1 β (31.2%, 22.7%, panel IV), IL-23 (63.3%, 21.8%, panel V), IL-32 α (69.5%, 86.1%, panel VI), TNF- α (100%, 83.4%, panel VII), and Gro- α (5.18%, 24.3%, panel VIII), respectively (Fig. 2A). Two of the A β -induced cytokines were reduced by insulin addition [IL-6 (48.5%) and IL-8 (15.4%)] but not by SP600125 addition (Fig. 2A, panels I and II), and one was reduced by SP600125 [GM-CSF (26.1%)] and not by insulin relative to A β alone (Fig. 2A, panel IX). Taken together, these results show that insulin and SP600125 treatments could reduce A β ₁₋₄₂-induced stimulation of all nine cytokines, a dramatic impact on the neuroinflammatory potential of A β and a probable mechanism of action for insulin and SP600125 protective effects against A β -induced cellular toxicity.

To validate the Cytokine Proteome ProfilerTM Arrays, two of the secreted cytokines, IL-8 and Gro- α , were analyzed by ELISA. IL-8 was significantly increased by A β ₁₋₄₂ treatment as compared to A β _{sc} peptide control (Fig. 2B, panel I). Insulin or SP600125 addition significantly decreased A β ₁₋₄₂-induced IL-8 expression (Fig. 2B, panel I, one-way ANOVA, Bonferroni's *post hoc* test, $*p < 0.05$). Levels of secreted Gro- α were significantly increased in iHBEC treated with A β ₁₋₄₂ peptide as compared to A β _{sc} peptide control, and were significantly reduced with the addition of SP600125 (Fig. 2B, panel II, one-way ANOVA, Bonferroni's *post hoc* test, $*p < 0.05$ and $**p < 0.001$, respectively). The treatments that include A β _{sc} validate that the effects are not due to presence of any

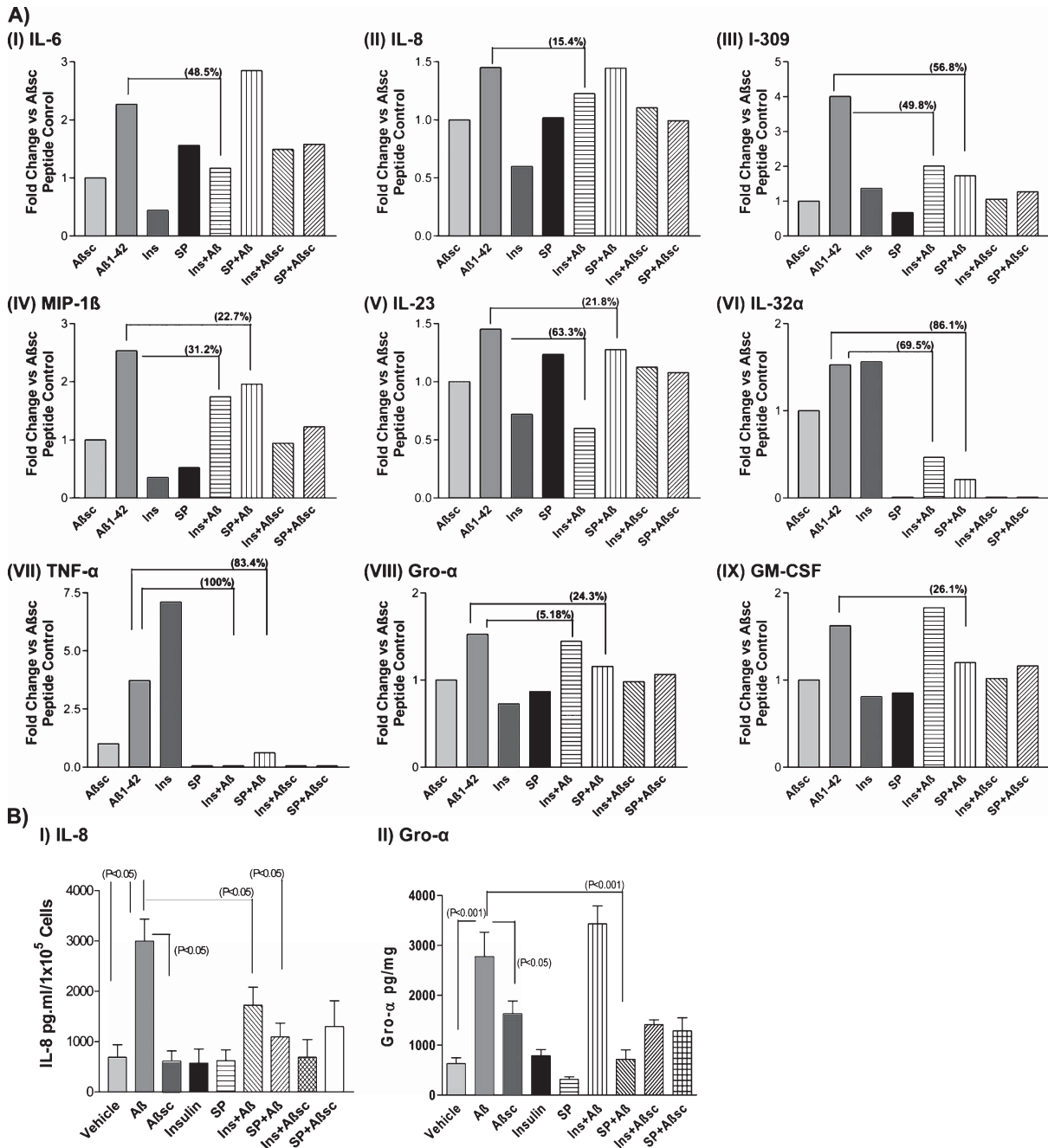


Fig. 2. Insulin and a JNK inhibitor SP600125 decrease A β ₁₋₄₂-induced cytokines in iHBEc. A) iHBEc were treated with A β ₁₋₄₂ (10 μ M), A β _{sc} peptide (10 μ M), insulin (1.7 μ M), and SP600125 (25 μ M) alone, or insulin and SP600125 in combination with A β peptides for 4 h. The conditioned media from three separate experiments were collected and the secreted cytokines were identified for each pooled ($n=3$) treatment group using a Human Cytokine Proteome Profiler™ Array. The immunoblot array spots, indicative of changes in multiple cytokines, were semi-quantified by densitometry and the results for each treatment are presented as a fold-change relative to A β _{sc} peptide control. B) iHBEc were treated as stated above and secreted protein levels for IL-8 and Gro- α were measured by ELISA. The data from three separate experiments were averaged and presented as IL-8 pg/ml/1 \times 10⁵ cells (panel I) or Gro- α pg/mg protein (panel II), one-way ANOVA, Bonferroni *post-hoc* test, ** $p < 0.001$, * $p < 0.05$. GM-CSF, granulocyte macrophage colony-stimulating factor; Gro, growth related oncogene; IL, interleukin; MIP, macrophage inflammatory protein; TNF, tumor necrosis factor.

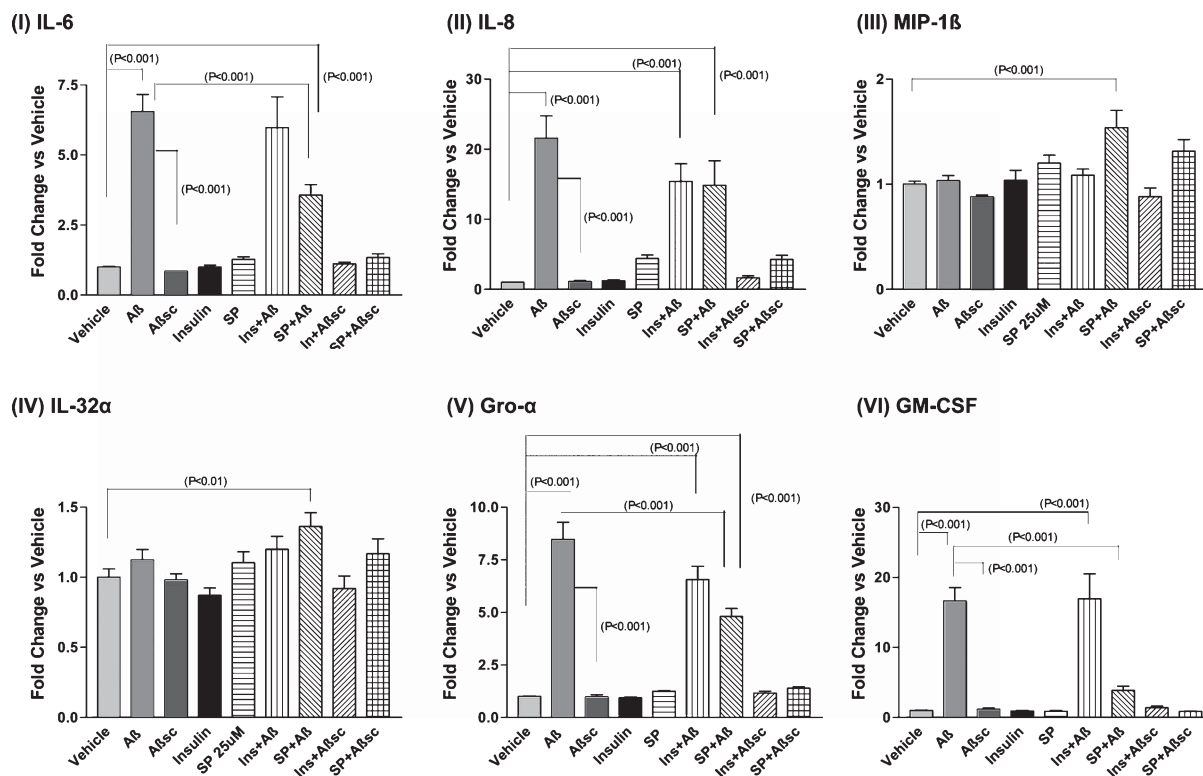


Fig. 3. Inhibition of JNK precludes A β ₁₋₄₂-induced inflammatory gene expression in iHBEC. A) iHBEC were treated with A β ₁₋₄₂ or A β _{sc} peptides (10 μ M), insulin (1.7 μ M), and SP600125 (25 μ M) alone or in combination with A β peptides for 4 h. QPCR analysis of select inflammatory genes was performed. The data from three separate experiments were averaged and presented as fold change relative to vehicle control for GM-CSF (panel I, ** p < 0.001), IL-6 (panel II, ** p < 0.001), IL-8 (panel III, * p < 0.001), Gro- α (panel IV, ** p < 0.001), MIP-1 β (panel V, ** p < 0.001), and IL-32 α (panel VI, ** p < 0.001). All data were analyzed by one-way ANOVA with Bonferroni's *post-hoc* test.

42-residue peptide. These data confirm that activation of insulin signaling, and reduction of JNK-AP1 signaling, can protect the cells from A β -induced inflammatory response.

Insulin and JNK inhibitor protect iHBEC cells from A β ₁₋₄₂-induced expression of inflammatory genes

To determine if A β ₁₋₄₂ would affect transcriptional events involved in the inflammatory response and whether insulin and SP600125 could be efficacious in altering the A β ₁₋₄₂-mediated response, cytokine gene expression was analyzed in treated iHBEC by qPCR. Previously, we showed that A β ₁₋₄₀ treatment of iHBEC stimulated IL-6, IL-8, and Gro- α gene expression [15]. Here, we show that A β ₁₋₄₂-induced inflammation stimulates an additional three genes (GM-CSF, MIP-1 β , and IL-32 α) and that inhibition of JNK by the addition of SP600125 significantly reduces A β ₁₋₄₂-mediated IL-6, IL-8, Gro- α , and GM-CSF inflammatory gene expression (Fig. 3, panels I,

II, V, and VI, one-way ANOVA, Bonferroni's *post-hoc* test, ** p < 0.001). MIP-1 β and IL-32 α gene expressions were not altered with A β ₁₋₄₂ treatment (Fig. 3, panels III and IV). SP600125 in combination with A β ₁₋₄₂ actually increased MIP-1 β and IL-32 α gene expression, but each independent stimulus did not (Fig. 3, panels III & IV, one-way ANOVA, Bonferroni's *post-hoc* test, ** p < 0.001, * p < 0.01). Insulin was unable to reduce the inflammatory gene expression induced by A β ₁₋₄₂ for all genes tested (compare A β ₁₋₄₂ + insulin to A β ₁₋₄₂). Importantly, A β _{sc} co-treatment with insulin or SP600125 resulted in similar cell responses as compared to insulin or SP600125 alone suggesting that the observed effects with A β ₁₋₄₂ were not due simply to the presence of a 42-mer peptide. These data suggest that insulin's protective effects against A β ₁₋₄₂-induced inflammatory response through the reduction of secreted cytokines is post-transcriptional in nature and that inhibition of JNK with SP600125 impacts gene expression at both the transcriptional and translational levels.

A β ₁₋₄₂ affects multiple transcription factors: consequences for insulin and JNK mediated signaling events

To gain a better understanding of the mechanisms of action that regulate signaling pathways in different iHBEC treatment conditions (A β ₁₋₄₂, insulin, and JNK inhibitor SP600125), we carried out TF profiling using a Combo Protein/DNA Array kit. The cells were treated with A β ₁₋₄₂, A β _{sc}, and insulin, alone or in combination with, A β peptides for 4 h. Pooled treatment conditions from three separate experiments were applied to the arrays and the data was presented for each independent TF normalized to A β _{sc} peptide control (set to 1, where significance was set at >2-fold change relative to A β _{sc}, as per manufacturers' instructions) (Table 3). The treatments uncovered a myriad of transcriptional changes and some very interesting relationships were revealed. The TFs were presented under three themes: shared pathways (Table 3A), divergent pathways (Tables 3B and 3C), and independent pathways (Supplementary Tables 2 and 3) with respect to A β ₁₋₄₂ and insulin.

First, seventeen TFs [PO-B, EBP-80, NF κ B(2), CBFb, NF-E1/YY1, SMAD3/4, AP-2(1), Stat-6, NF-Atx, MRE, CREB-BP1, PIT-1(1), PRD1-BFc, GR/PR, Stat-5b, HSE, MEF-1(1)] displayed significant increases, relative to A β _{sc}, when iHBEC was treated independently with either A β ₁₋₄₂ or insulin (Table 3A, top). This is interesting as it shows that insulin and A β stimulate certain common pathways. Among these 17 TFs, six of them [NF κ B(2), SMAD3/4, MRE, Stat-5b, HSE, and MEF-1] were markedly decreased relative to A β ₁₋₄₂ or insulin when A β ₁₋₄₂ and insulin were added in combination (Table 3A, top). This suggests that hyper-stimulation of the pathways might occur; perhaps creating a temporal shift due to maximal signaling thresholds being reached sooner by "double dosing" the same signaling pathway and enhancing negative feedback inhibitor mechanisms for these TFs. Seven of the 17 TFs [PO-B, AP-2 (1), Stat-6, NF-Atx, CREB-BP-1, Pit-1(1), and GR/PR] that were increased as a result of either A β ₁₋₄₂ or insulin treatment independently were increased further relative to A β ₁₋₄₂ or insulin when A β ₁₋₄₂ and insulin were added in combination, suggesting a synergistic influence on these pathways (Table 3A, top). These may represent some of the potential mechanisms whereby the presence of A β peptides results in over-stimulation of the insulin-induced signaling pathways. Western blot analysis of phospho-IR and phospho-AKT showed that insulin

signaling was not increased with the addition of A β ₁₋₄₂ relative to insulin alone (Supplementary Figure 1B and C, one-way ANOVA, Bonferroni's *post-hoc* test, * p < 0.05, ** p < 0.01, *** p < 0.001). Three TFs that increased with both treatments independently did not respond differentially with combination treatment of A β ₁₋₄₂ and insulin (EBP-80, CBFb, and NF-E1/YY1, Table 3A, top). Five TFs, namely MBP-1, DE-1, GKLF, AR, and PPAR (3), were markedly decreased with either A β ₁₋₄₂ or insulin treatment (Table 3A, bottom). Comparing the response from A β _{sc} + insulin treatment to insulin treatment alone shows that the A β ₁₋₄₂ effects are not simply due to the presence of a 42-mer peptide. Second, there were 15 TFs [ETS(1), Stat-3, LyF(1), XBP-1, MBP-1(1), RFX-1/2/3(2), LFAi(2), PAX-5, p53(1), NF κ B(1), CD23RC(1), KPF-1, E2F-1(1), and EKLF(1)] that were decreased as a result of A β ₁₋₄₂ treatment but increased in the presence of insulin, relative to A β _{sc}, illustrating a divergent pathway relationship effect (Table 3B). These could be the pathways in which insulin can exert protective effects against A β -mediated toxicities and circumvent neuroinflammation, as suggested by co-treatment with A β ₁₋₄₂ and insulin relative to A β ₁₋₄₂ treatment. Again, that treatment of A β _{sc} + insulin resulted in similar TF responses to insulin treatment alone suggest that changes elicited as a result of A β ₁₋₄₂ treatment were not due to peptide effects. Third, also very interesting was the finding that 30 TFs were independently increased with insulin treatment alone (Supplementary Table 2). These are interesting pathways that can be explored as biomarkers for insulin therapies or possible therapeutic targets for diabetes.

Four TFs, namely GR/PR, AP-2(1), Pit-1(1), and Stat-6, were increased as a result of A β ₁₋₄₂ treatment but decreased by SP600125, illustrating divergent pathway effects of A β and SP600125 (Table 3C, top). There were also 11 TFs that were decreased by A β ₁₋₄₂ but increased as a result of SP600125 treatment, namely TFE3, EGR-2, ZNF174, E2F-1(1), X2 BP, Myc-Max, PEBP-2, OCT(1), CEBP(5), HiNF/D3, and MEF-2(1) (Table 3C, bottom). These TFs represent possible mechanisms for SP600125-mediated protection against A β ₁₋₄₂ cellular insults, as suggested with A β ₁₋₄₂+SP600125 compared to A β ₁₋₄₂ treatment. Importantly, that A β _{sc}+SP600125 resulted in similar effect to SP600125 treatment alone showed that the A β ₁₋₄₂ results were not due to generic peptide effects. There were also 85 TFs that were grouped as A β ₁₋₄₂ independent pathways in that they were only affected by A β ₁₋₄₂ treatment; 2 TFs [Surf-2 (2) and ABF-1] were increased with A β ₁₋₄₂ treatment

Table 3

Statistically significant TF changes. The iHBEC were treated with either A β _{sc}, A β ₁₋₄₂ or insulin alone or in combination with A β peptides for 4 h and the nuclear material was harvested. This was performed three independent times, the treatment conditions were pooled, and each treatment was applied to a TF array. The arrays were semi-quantified by densitometry and the TFs were presented relative to A β _{sc} (set to 1) and organized by their response to A β , insulin, and SP600125. The TFs that increased or decreased for both insulin and A β ₁₋₄₂ were organized in the 'shared' pathways (Table 3A), those that increased with insulin and decreased by A β ₁₋₄₂ were organized in the 'divergent' pathways (Table 3B), and those that increased with insulin and decreased by SP600125 (or vice versa) were 'displayed' in divergent pathways (Table 3C). TFs that were affected only by either insulin or A β ₁₋₄₂ ('independent' pathways) were organized into Supplementary Tables 2 and 3, respectively

(A) Shared pathways

TF	A β	Ins	Ins + A β	Ins + A β _{sc}
<i>Fold change versus Aβ_{sc} – Up Aβ₁₋₄₂ and insulin</i>				
PO-B	2.8	4.5	5.5	4.9
EBP-80	2.6	3.4	3.6	2.4
NF κ B(2)	2.1	3.2	0.1	1.8
CBFB	2.1	2.5	2.3	3.5
NF-E1/YY1	2.6	3.9	3.5	5.0
SMAD 3/4	17.2	22.5	15.1	28.1
AP-2(1)	2.6	16.4	28.8	18.5
Stat 6	2.2	12.6	16.8	20.5
NF-Atx	3.6	4.4	16.5	6.5
MRE	22.7	33.1	19.8	40.0
CREB-BP1	5.4	13.9	40.0	20.7
Pit-1(1)	5.3	26.1	28.2	44.7
PRD1-BFc	29.3	30.5	26.6	36.0
GR/PR	2.6	18.7	27.1	36.4
Stat-5b	52.2	21.7	9.9	25.5
HSE	81.8	86.2	40.3	166.5
MEF-1(1)	32.8	49.1	1.0	57.8
<i>Fold change versus Aβ_{sc} – down Aβ₁₋₄₂ and insulin</i>				
MBP-1(2)	0.1	0.4	0.2	0.4
DE-1	0.1	0.4	0.2	0.7
GKLF	0.2	0.2	0.2	0.3
AR	0.2	0.4	0.8	0.3
PPAR(3)	0.2	0.2	0.7	0.4

(B) Divergent pathways

TF	A β	Ins	Ins + A β	Ins + A β _{sc}
<i>Fold change versus Aβ_{sc} – down Aβ₁₋₄₂, up insulin</i>				
ETS(1)	0.0	2.0	1.8	2.3
Stat-3	0.0	2.5	2.4	3.9
LyF(1)	0.2	2.2	1.5	2.4
XBP-1	0.3	3.2	1.1	3.3
MBP-1(1)	0.1	2.3	0.8	2.6
RFX-1/2/3(2)	0.2	2.5	1.0	3.8
LF-Ai(2)	0.3	2.0	0.8	1.1
PAX-5	0.4	2.1	1.6	2.9
p53(1)	0.1	3.9	4.2	6.7
NF κ B(1)	0.1	3.5	10.4	4.7
CD28RC(1)	0.2	5.6	2.7	5.2
KPF-1	0.3	6.6	3.5	7.5
E2F-1(1)	0.3	3.9	1.7	6.1
EKLF(1)	0.1	4.0	3.0	7.0

(C) Divergent pathways

TF	A β	SP	SP + A β	SP + A β _{sc}
<i>Fold change versus Aβ_{sc} – up Aβ₁₋₄₂, down SP</i>				
GR/PR	2.6	0.2	0.2	0.7
AP-2(1)	2.6	0.1	0.1	0.7
Pit-1(1)	5.3	0.0	1.1	0.5
Stat 6	2.2	0.1	2.0	0.4

Table 3
(Continued)

TF	A β	SP	SP + A β	SP + A β_{sc}
<i>Fold change versus Aβ_{sc} – down Aβ_{1-42}, up SP</i>				
TFE3	0.4	3.0	1.8	1.7
EGR-2	0.0	3.5	0.8	2.3
ZNF174	0.4	2.8	0.7	2.9
E2F-1(1)	0.3	3.9	1.7	6.1
X2 BP	0.3	2.2	0.5	1.6
Myc-Max	0.3	2.2	1.5	1.4
PEBP-2	0.3	6.8	2.2	2.8
OCT(1)	0.0	5.1	4.8	6.5
CEBP(5)	0.1	5.6	2.3	4.0
HiNF/D3	0.5	12.4	2.4	8.7
MEF-2(1)	0.5	8.1	1.8	5.6

Of note, the following so-called TFs actually name the DNA binding sequence: PO-B, MRE, HSE, DE-1, and ETS [51–55].

(Supplementary Table 3, top) whereas 83 of those TFs were downregulated with A β_{1-42} treatment (Supplementary Table 3, bottom). These TFs could offer other targets for therapeutic intervention. Notably, the description of each TF and its reported involvement with insulin, JNK, and AD were presented in the Supplementary Table 4. We also attempted to functionally categorize the TFs listed in the A β_{1-42} and insulin shared and divergent pathways (Supplementary Figure 2).

To validate the TF array, western blot analyses were performed on phosphorylated inhibitory molecules of two TFs from whole cell lysates after cell treatment. NF κ B exists in the cytoplasm during resting state; upon cellular stimuli the inhibitor of NF κ B (I κ B) is phosphorylated (and subsequently degraded) while NF κ B translocates to the nucleus to induce gene expression [37]. Phospho-I κ B was detected in A β_{1-42} - and insulin-treated cells relative to A β_{sc} -treated cells (Fig. 4A, left panel). A β_{1-42} and insulin treatment both phosphorylate I κ B independently which is in accordance with both treatments stimulating NF κ B, as determined from the TF array (Fig. 4A, right panel). Binding of the retinoblastoma tumor suppressor protein (pRb) to E2F1 prevents transcriptional activation while phosphorylation of pRb releases E2F1 allowing initiation of gene expression [38]. A β_{1-42} treatment had no significant impact on pRb phosphorylation while insulin treatment significantly increased phosphorylation relative to A β_{sc} treatment (Fig. 4B, left panel, one-way ANOVA, Bonferroni's *post hoc* test, * $p < 0.05$ and ** $p < 0.001$). These data are in accordance with the TF array results for E2F1 (Fig. 4B, right panel) wherein A β_{1-42} reduces while insulin treatment increases E2F1 activation (A β_{1-42} and insulin treatment elicit a divergent response on E2F1). These data provide validation for the TF array results.

Combined insulin and SP600125 treatment offers synergistic advantages in reducing A β_{1-42} -induced JNK activation

We have shown that treatment with insulin or SP600125 can reduce A β -induced toxicity, cytokine secretion, cytokine gene expression, and TF changes. We next wanted to determine if insulin and SP600125, given in combination, would be more efficacious in reducing inflammatory signaling pathways. The iHBEc was treated with up to 25 μ M of SP600125 alone or in combination with A β_{1-42} (or A β_{sc}) and/or insulin for 4 h. JNK-AP1 activation was monitored by examination of c-Jun ser63 phosphorylation by immunoblot analysis (Fig. 5A). SP600125 significantly decreased A β_{1-42} -induced c-Jun ser63 phosphorylation at 10 and 25 μ M (Fig. 5B, unpaired two-tailed *t*-test ** $p < 0.00313$, ** $p < 0.0085$). Interestingly, neither 1 μ M SP600125 nor 1.7 μ M insulin was effective at reducing A β_{1-42} phosphorylation of c-Jun ser63, but SP600125 at 1 μ M given in combination with 1.7 μ M insulin significantly reduced A β -induced c-Jun ser63 phosphorylation; the combined treatment was significantly more efficacious (Fig. 5B, unpaired two-tailed *t*-test ** $p < 0.0146$). This reduction in A β_{1-42} -induced c-Jun ser63 phosphorylation with the combination of 1 μ M SP600125 and 1.7 μ M insulin was not due to the presence of a 42-mer peptide (compare A β_{sc} +ins+SP1 to A β +ins+SP1). However, at higher doses of SP600125 (25 μ M) there was no difference in c-Jun ser63 phosphorylation between A β +ins+SP and A β_{sc} +ins+SP (Supplementary Figure 1A). The data were analyzed by unpaired two-tailed *t*-test. These data show that insulin treatment and JNK inhibitor may synergistically enhance insulin signaling and suppress A β -evoked signaling, which leads to reduced AP-1 activation and inflammatory response.

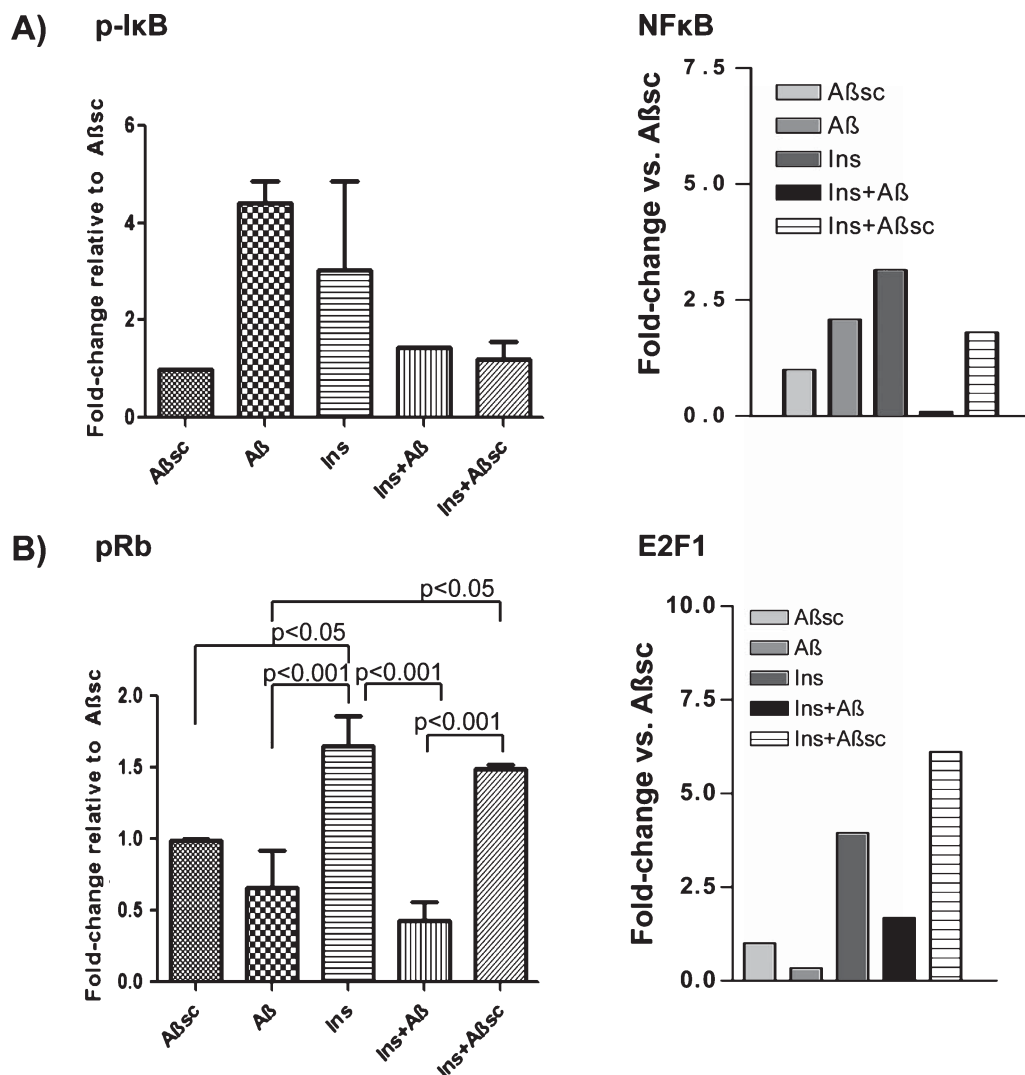


Fig. 4. Validation of TF array. Cells were treated with A β sc, A β ₁₋₄₂ peptides (10 μ M), and insulin (1.7 μ M) independently or in combination for 4 h. Cell-proteins were resolved by SDS-PAGE, transferred to PVDF membrane, and immunoblotted for p-I κ B (A, left panel) and p-Rb (B, right panel). The bands were semi-quantified by densitometry analysis and normalized to actin. The data from two-three separate experiments were averaged and presented relative to A β sc peptide control (One-way ANOVA, Bonferroni *post-hoc* test, * p < 0.05, ** p < 0.001). The TF array results for NF κ B(2) (A, right panel) and E2F-1 (B, right panel) taken from Tables 3A (top) and Table 3B, respectively, are shown.

DISCUSSION

The data presented here exemplify some very interesting concepts. A β ₁₋₄₂ induces toxicity in iHBEC mediated by cytokines showing that human cerebral vascular cells can be compromised by excess of this peptide. A β ₁₋₄₂ stimulates the inflammatory response by both transcriptional and post-transcriptional events. Interestingly, all of the A β ₁₋₄₂-induced cytokines could be reduced by insulin and SP600125 treatment showing that therapeutic targeting through the

enhancement of insulin signaling and inhibition of JNK pathways could alleviate A β -induced inflammatory response. Many of the cytokines (IL-6, IL-8, MIP-1 β , TNF- α , Gro- α , and GM-CSF) that were increased by A β ₁₋₄₂ in these human brain endothelial cells were previously reported to be increased by A β deposition in various cell types [15, 39, 40] and/or in AD brain tissue [39, 41]. An *in vivo* study with IL-23 and an *ex vivo* study with IL-32 suggested a role for these cytokines in neurodegenerative and neuroinflammatory diseases such as AD [42, 43]. There are no reports of I-309 acti-

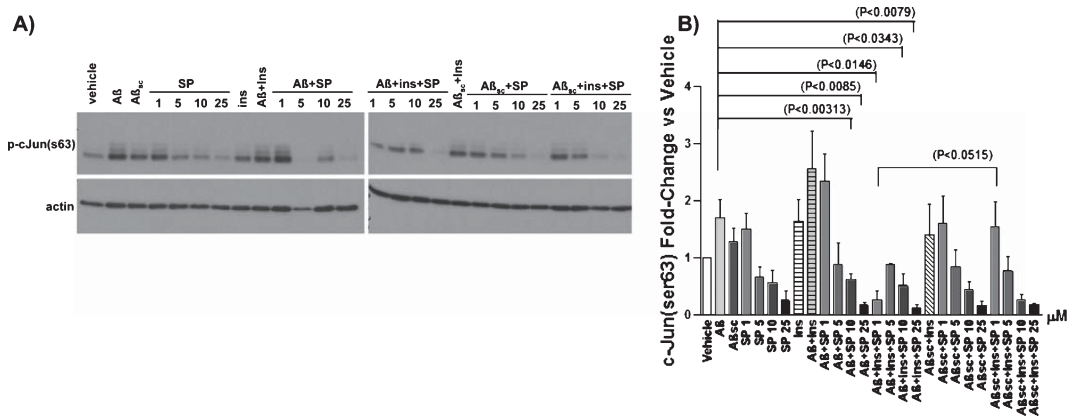


Fig. 5. Insulin in combination with SP600125 offers synergistic advantages in preventing A β_{1-42} -induced JNK activation and c-Jun phosphorylation. iHBEC were treated with A β_{1-42} (10 μ M), A β_{sc} peptide (10 μ M), insulin (1.7 μ M), and SP600125 at various concentrations (1, 5, 10, 25 μ M) alone or in combination for 4 h. Cell proteins were resolved by SDS-PAGE, transferred to PVDF membranes and incubated with c-Jun Ser 63-specific antibody and the image was visualized by chemiluminescence and captured on film (A). The bands were semi-quantified by densitometry and normalized to actin. The data from three separate experiments were averaged and presented as fold-change compared to vehicle (B, ** $p < 0.00313$, ** $p < 0.0085$, * $p < 0.0146$, * $p < 0.0343$, ** $p < 0.0079$, unpaired two-tailed t -test).

vation in *in vitro* or *in vivo* AD models, but recently, it was shown to be a novel CSF biomarker for AD [44]. Insulin has been shown to exert anti-inflammatory effects at low doses [45, 46]. Although insulin addition reduced the levels of the secreted cytokines (except that of GM-CSF) as compared to A β_{1-42} treatment, none of the tested cytokines displayed reduced expression with the addition of insulin. It is possible that significant changes in gene expression occurred at earlier time points (<4 h). TNF- α , which is involved in inducing insulin resistance [4, 47], was increased from cells treated with either A β or insulin (Fig. 2B, VII), but was markedly reduced in the presence of both A β and insulin. This can be explained in the following way, in the presence of infectious agents, the induced TNF- α is part of the inflammatory response from the cells, and in the absence of A β peptides (or infectious agents), insulin-induced TNF- α may play a role as a negative feedback mechanism to limit or regulate insulin signaling. Addition of insulin to the cells may suppress A β -induced inflammatory response including TNF- α . This assumption requires further investigation. The current data suggest that insulin's protective properties on cytokine expression act at the post-transcriptional level.

JNK is reported to be involved in the induction of proinflammatory cytokines; pharmacological inhibition of JNK (including SP600125) has been demonstrated to attenuate the release of pro-inflammatory cytokines [48]. The addition of SP600125 reduced the secreted levels of seven of the nine A β -stimulated cytokines. QPCR analysis revealed that only two

of these reductions (Gro- α and GM-CSF) resulted from a decrease in gene expression. A β + SP600125 treatment actually increased the gene expression of MIP-1 β and IL-32 α (even though the secreted levels were decreased). This was surprising considering SP600125, similar to Dalesconols B [49], is an anti-inflammatory agent. Importantly, the comparison of SP+A β treatment to SP+A β_{sc} treatment is not significant suggesting that the increase observed with SP+A β relative to vehicle was due to non-specific peptide effects in combination with SP600125. Although not changed in the conditioned media, SP600125 addition reduced the expression of IL-6 and IL-8. Thus, inhibition of JNK exerts influence on both transcriptional and post-transcriptional events.

SP600125 was originally reported to inhibit JNK2 activity; however, more recent data has shown that 13 of 30 tested protein kinases were inhibited by 10 μ M SP600125 at various degrees [50]. Thus, some of the observations from SP600125 treatment in this study may be due to the inhibition of other protein kinases. Altogether, the cytokine and qPCR findings suggest that insulin and SP600125 are efficacious at restoring insulin signaling and reducing all A β_{1-42} -induced inflammatory signaling events in iHBEC.

TF array profiling showed the pleiotropic influence A β peptides have on multiple cellular signaling pathways and revealed several common and divergent signaling pathways induced by A β , insulin, and SP600125. The findings from the TF array were classified into three main categories: 1) TFs that both insulin and A β_{1-42} either increased or decreased (shared path-

ways); 2) TFs that A β ₁₋₄₂ and insulin (or SP600125) both changed but in opposite directions (divergent pathways); and 3) TFs that were only changed by either A β ₁₋₄₂ or insulin (independent pathways). With respect to the shared pathways, i) some of the TFs that were upregulated with A β or insulin treatment alone, were not significantly increased in combination; and ii) for some TFs, co-stimulation with insulin and A β , resulted in hyperstimulation. These data support the notion that A β dysregulates insulin signaling, which may lead to insulin resistance in AD brain. In the former case, this suggested that A β and insulin overstimulation was reached at an earlier time point followed by the onset of feedback mechanisms resulting in hypostimulation at the time of analysis or A β -mediated insulin resistance. For instance, MEF-1 was stimulated by 32-fold and 49-fold with A β ₁₋₄₂ or insulin alone, respectively; however, the combination of A β + insulin resulted in a 96% reduction relative to baseline. In the latter case, this suggested that A β and insulin hyperstimulated the pathways but thresholds had not yet been reached to turn on negative feedback regulatory mechanisms for these pathways. TFs that fall under the divergent pathway classification also include A β and SP600125. Depending on their beneficial or deleterious effect of downstream targets, these TFs could potentially be regulated by pharmacological intervention to obtain desired outcomes. There were, however, 85 TFs that were changing with A β but not with insulin. These highlight some of the A β ₁₋₄₂-induced pathways that do not involve insulin dysregulation. Importantly, the cytokine array for treated iHBEC showed that insulin and SP600125 reduced all the A β ₁₋₄₂-induced inflammatory cytokines, thus these A β +insulin/SP600125 shared and divergent pathways highlight therapeutic targets to restore insulin signaling, inhibit A β -induced inflammatory response, and potentially impede the progression of AD.

The iHBEC combinatorial treatment assessment revealed that low dose SP600125 (1 μ M) alone was unable to reduce A β -induced inflammatory response, as evidenced by c-Jun p63 phosphorylation, but that the combination of insulin along with low dose SP600125 reduced the A β -evoked inflammatory response. Combination treatments with docosahexaenoic acid (a JNK inhibitor) and curcumin (a turmeric component that attenuates A β and JNK activation) have been reported that improve insulin signaling and cognitive deficits in AD [26]. We showed that the combination of increasing insulin signaling and reducing A β -induced inflammation was more efficacious than only trying to reduce JNK activation.

In summary, this study sheds light on gene expression and signaling pathways involved with A β , insulin, and anti-inflammatory JNK inhibitor SP600125. A β and insulin can affect many shared signaling pathways in cells, and A β may thus dysregulate insulin signaling, contributing to insulin resistance. Both insulin and the JNK inhibitor SP600125 can alleviate A β -evoked inflammatory response independently. However, by activation of insulin signaling and JNK inhibition in combination, we may more efficaciously reverse A β -induced cytotoxicity, insulin dysregulation, and inflammatory response. We hope that the categorization of the extensive transcription factor profiling from various cell conditions will be a stepping stone for researchers in determining pathways to target for therapeutic intervention.

ACKNOWLEDGMENTS

This study was supported by funding from the National Research Council Canada and CIHR grants (#109606 to W. Zhang and Z. Yang; #106886 and CIHR# TAD 125698 to W. Zhang). The authors would like to thank Dr. P-O. Couraud for supplying the immortalized human brain endothelial cells, hCMEC/D3, used in this study. The authors would also like to thank Dr. Yue Chen at the University of Ottawa for advice on statistical analyses and Dr. Yu Zeng for her technical assistance.

Authors' disclosures available online (<http://www.j-alz.com/disclosures/view.php?id=2012>).

SUPPLEMENTARY MATERIAL

Supplementary tables are available in the electronic version of this article: <http://dx.doi.org/10.3233/JAD-131949>.

REFERENCES

- [1] Ott A, Stolk RP, van Harskamp F, Pols HA, Hofman A, Breteler MM (1999) Diabetes mellitus and the risk of dementia: The Rotterdam Study. *Neurology* **53**, 1937-1942.
- [2] Ferreira ST, Klein WL (2011) The Abeta oligomer hypothesis for synapse failure and memory loss in Alzheimer's disease. *Neurobiol Learn Mem* **96**, 529-543.
- [3] de la Monte SM (2009) Insulin resistance and Alzheimer's disease. *BMB Rep* **42**, 475-481.
- [4] Bomfim TR, Fornly-Germano L, Sathler LB, Brito-Moreira J, Houzel JC, Decker H, Silverman MA, Kazi H, Melo HM, McClean PL, Holscher C, Arnold SE, Talbot K, Klein WL, Munoz DP, Ferreira ST, De Felice FG (2012) An anti-diabetes agent protects the mouse brain from defective insulin

- signaling caused by Alzheimer's disease-associated A β oligomers. *J Clin Invest* **122**, 1339-1353.
- [5] Talbot K, Wang HY, Kazi H, Han LY, Bakshi KP, Stucky A, Fuino RL, Kawaguchi KR, Samoyedny AJ, Wilson RS, Arvanitakis Z, Schneider JA, Wolf BA, Bennett DA, Trojanowski JQ, Arnold SE (2012) Demonstrated brain insulin resistance in Alzheimer's disease patients is associated with IGF-1 resistance, IRS-1 dysregulation, and cognitive decline. *J Clin Invest* **122**, 1316-1338.
- [6] Erol A (2009) Unraveling the molecular mechanisms behind the metabolic basis of sporadic Alzheimer's disease. *J Alzheimers Dis* **17**, 267-276.
- [7] Keller JN, Pang Z, Geddes JW, Begley JG, Germeyer A, Waeg G, Mattson MP (1997) Impairment of glucose and glutamate transport and induction of mitochondrial oxidative stress and dysfunction in synaptosomes by amyloid beta-peptide: Role of the lipid peroxidation product 4-hydroxynonenal. *J Neurochem* **69**, 273-284.
- [8] Xie L, Helmerhorst E, Taddei K, Plewright B, Van Bronswijk W, Martins R (2002) Alzheimer's beta-amyloid peptides compete for insulin binding to the insulin receptor. *J Neurosci* **22**, RC221.
- [9] Farris W, Mansourian S, Chang Y, Lindsley L, Eckman EA, Froesch MP, Eckman CB, Tanzi RE, Selkoe DJ, Guenette S (2003) Insulin-degrading enzyme regulates the levels of insulin, amyloid beta-protein, and the beta-amyloid precursor protein intracellular domain *in vivo*. *Proc Natl Acad Sci U S A* **100**, 4162-4167.
- [10] Qin W, Jia J (2008) Down-regulation of insulin-degrading enzyme by presenilin 1 V97L mutant potentially underlies increased levels of amyloid beta 42. *Eur J Neurosci* **27**, 2425-2432.
- [11] LaFerla FM, Green KN, Oddo S (2007) Intracellular amyloid-beta in Alzheimer's disease. *Nat Rev Neurosci* **8**, 499-509.
- [12] Bell RD, Zlokovic BV (2009) Neurovascular mechanisms and blood-brain barrier disorder in Alzheimer's disease. *Acta Neuropathol* **118**, 103-113.
- [13] Aguirre V, Uchida T, Yenush L, Davis R, White MF (2000) The c-Jun NH(2)-terminal kinase promotes insulin resistance during association with insulin receptor substrate-1 and phosphorylation of Ser(307). *J Biol Chem* **275**, 9047-9054.
- [14] Kaneto H (2005) The JNK pathway as a therapeutic target for diabetes. *Expert Opin Ther Targets* **9**, 581-592.
- [15] Vukic V, Callaghan D, Walker D, Lue LF, Liu QY, Couraud PO, Romero IA, Weksler B, Stanimirovic DB, Zhang W (2009) Expression of inflammatory genes induced by beta-amyloid peptides in human brain endothelial cells and in Alzheimer's brain is mediated by the JNK-API signaling pathway. *Neurobiol Dis* **34**, 95-106.
- [16] Li M, Shang DS, Zhao WD, Tian L, Li B, Fang WG, Zhu L, Man SM, Chen YH (2009) Amyloid beta interaction with receptor for advanced glycation end products up-regulates brain endothelial CCR5 expression and promotes T cells crossing the blood-brain barrier. *J Immunol* **182**, 5778-5788.
- [17] Du H, Li P, Wang J, Qing X, Li W (2012) The interaction of amyloid beta and the receptor for advanced glycation endproducts induces matrix metalloproteinase-2 expression in brain endothelial cells. *Cell Mol Neurobiol* **32**, 141-147.
- [18] Tu YF, Tsai YS, Wang LW, Wu HC, Huang CC, Ho CJ (2011) Overweight worsens apoptosis, neuroinflammation and blood-brain barrier damage after hypoxic ischemia in neonatal brain through JNK hyperactivation. *J Neuroinflammation* **8**, 40.
- [19] Pang T, Wang J, Benicky J, Sanchez-Lemus E, Saavedra JM (2012) Telmisartan directly ameliorates the neuronal inflammatory response to IL-1beta partly through the JNK/c-Jun and NADPH oxidase pathways. *J Neuroinflammation* **9**, 102.
- [20] Leow-Dyke S, Allen C, Denes A, Nilsson O, Maysami S, Bowie AG, Rothwell NJ, Pinteaux E (2012) Neuronal toll-like receptor 4 signaling induces brain endothelial activation and neutrophil transmigration *in vitro*. *J Neuroinflammation* **9**, 230.
- [21] Xiong H, Callaghan D, Jones A, Bai J, Rasquinha I, Smith C, Pei K, Walker D, Lue LF, Stanimirovic D, Zhang W (2009) ABCG2 is upregulated in Alzheimer's brain with cerebral amyloid angiopathy and may act as a gatekeeper at the blood-brain barrier for A β (1-40) peptides. *J Neurosci* **29**, 5463-5475.
- [22] Exalto LG, Whitmer RA, Kappele LJ, Biessels GJ (2012) An update on type 2 diabetes, vascular dementia and Alzheimer's disease. *Exp Gerontol* **47**, 858-864.
- [23] Weksler BB, Subileau EA, Perriere N, Charneau P, Holloway K, Leveque M, Tricoire-Leignel H, Nicotra A, Bourdoulous S, Turowski P, Male DK, Roux F, Greenwood J, Romero IA, Couraud PO (2005) Blood-brain barrier-specific properties of a human adult brain endothelial cell line. *FASEB J* **19**, 1872-1874.
- [24] Huang da W, Sherman BT, Lempicki RA (2009) Systematic and integrative analysis of large gene lists using DAVID bioinformatics resources. *Nat Protoc* **4**, 44-57.
- [25] Karin M, Liu Z, Zandi E (1997) AP-1 function and regulation. *Curr Opin Cell Biol* **9**, 240-246.
- [26] Ma QL, Yang F, Rosario ER, Ubeda OJ, Beech W, Gant DJ, Chen PP, Hudspeth B, Chen C, Zhao Y, Vinters HV, Frautschy SA, Cole GM (2009) Beta-amyloid oligomers induce phosphorylation of tau and inactivation of insulin receptor substrate via c-Jun N-terminal kinase signaling: Suppression by omega-3 fatty acids and curcumin. *J Neurosci* **29**, 9078-9089.
- [27] Reed T, Perluigi M, Sultana R, Pierce WM, Klein JB, Turner DM, Coccia R, Markesbery WR, Butterfield DA (2008) Redox proteomic identification of 4-hydroxy-2-nonenal-modified brain proteins in amnesic mild cognitive impairment: Insight into the role of lipid peroxidation in the progression and pathogenesis of Alzheimer's disease. *Neurobiol Dis* **30**, 107-120.
- [28] Noshita T, Murayama N, Oka T, Ogino R, Nakamura S, Inoue T (2012) Effect of bFGF on neuronal damage induced by sequential treatment of amyloid beta and excitatory amino acid *in vitro* and *in vivo*. *Eur J Pharmacol* **695**, 76-82.
- [29] Jarvis K, Assis-Nascimento P, Mudd LM, Montague JR (2007) Beta-amyloid toxicity and reversal in embryonic rat septal neurons. *Neurosci Lett* **423**, 184-188.
- [30] Feng C, Zhang C, Shao X, Liu Q, Qian Y, Feng L, Chen J, Zha Y, Zhang Q, Jiang X (2012) Enhancement of nose-to-brain delivery of basic fibroblast growth factor for improving rat memory impairments induced by co-injection of beta-amyloid and ibotenic acid into the bilateral hippocampus. *Int J Pharm* **423**, 226-234.
- [31] Verdoliva A, Riviaccio V, Rossi M (2010) Simplified beta-amyloid peptides for safer Alzheimer's vaccines development. *Hum Vaccin* **6**, 936-947.
- [32] Haglund M, Kalaria R, Slade JY, Englund E (2006) Differential deposition of amyloid beta peptides in cerebral amyloid angiopathy associated with Alzheimer's disease and vascular dementia. *Acta Neuropathol* **111**, 430-435.
- [33] Gravina SA, Ho L, Eckman CB, Long KE, Otvos L Jr, Younkin LH, Suzuki N, Younkin SG (1995) Amyloid beta

- protein (A beta) in Alzheimer's disease brain. Biochemical and immunocytochemical analysis with antibodies specific for forms ending at A beta 40 or A beta 42(43). *J Biol Chem* **270**, 7013-7016.
- [34] Jellinger KA (2002) Alzheimer disease and cerebrovascular pathology: An update. *J Neural Transm* **109**, 813-836.
- [35] Tai LM, Holloway KA, Male DK, Loughlin AJ, Romero IA (2010) Amyloid-beta-induced occludin down-regulation and increased permeability in human brain endothelial cells is mediated by MAPK activation. *J Cell Mol Med* **14**, 1101-1112.
- [36] Kania KD, Wijesuriya HC, Hladky SB, Barrand MA (2011) Beta amyloid effects on expression of multidrug efflux transporters in brain endothelial cells. *Brain Res* **1418**, 1-11.
- [37] Viatour P, Merville MP, Bours V, Chariot A (2005) Phosphorylation of NF-kappaB and IkappaB proteins: Implications in cancer and inflammation. *Trends Biochem Sci* **30**, 43-52.
- [38] Dick FA, Dyson N (2003) pRB contains an E2F1-specific binding domain that allows E2F1-induced apoptosis to be regulated separately from other E2F activities. *Mol Cell* **12**, 639-649.
- [39] Xia MQ, Hyman BT (1999) Chemokines/chemokine receptors in the central nervous system and Alzheimer's disease. *J Neurovirol* **5**, 32-41.
- [40] Forloni G, Mangiarotti F, Angeretti N, Lucca E, De Simoni MG (1997) Beta-amyloid fragment potentiates IL-6 and TNF-alpha secretion by LPS in astrocytes but not in microglia. *Cytokine* **9**, 759-762.
- [41] Rubio-Perez JM, Morillas-Ruiz JM (2012) A review: Inflammatory process in Alzheimer's disease, role of cytokines. *ScientificWorldJournal* **2012**, 756357.
- [42] Vom Berg J, Prokop S, Miller KR, Obst J, Kalin RE, Lopategui-Cabezas I, Wegner A, Mair F, Schipke CG, Peters O, Winter Y, Becher B, Heppner FL (2012) Inhibition of IL-12/IL-23 signaling reduces Alzheimer's disease-like pathology and cognitive decline. *Nat Med* **18**, 1812-1819.
- [43] Cho KS, Park SH, Joo SH, Kim SH, Shin CY (2010) The effects of IL-32 on the inflammatory activation of cultured rat primary astrocytes. *Biochem Biophys Res Commun* **402**, 48-53.
- [44] Hu WT, Chen-Plotkin A, Arnold SE, Grossman M, Clark CM, Shaw LM, Pickering E, Kuhn M, Chen Y, McCluskey L, Elman L, Karlawish J, Hurtig HI, Siderowf A, Lee VM, Soares H, Trojanowski JQ (2010) Novel CSF biomarkers for Alzheimer's disease and mild cognitive impairment. *Acta Neuropathol* **119**, 669-678.
- [45] Fishel MA, Watson GS, Montine TJ, Wang Q, Green PS, Kulstad JJ, Cook DG, Peskind ER, Baker LD, Goldgaber D, Nie W, Asthana S, Plymate SR, Schwartz MW, Craft S (2005) Hyperinsulinemia provokes synchronous increases in central inflammation and beta-amyloid in normal adults. *Arch Neurol* **62**, 1539-1544.
- [46] Dandona P (2002) Endothelium, inflammation, and diabetes. *Curr Diab Rep* **2**, 311-315.
- [47] Clark I, Atwood C, Bowen R, Paz-Filho G, Vissel B (2012) Tumor necrosis factor-induced cerebral insulin resistance in Alzheimer's disease links numerous treatment rationales. *Pharmacol Rev* **64**, 1004-1026.
- [48] Mehan S, Meena H, Sharma D, Sankhla R (2011) JNK: A stress-activated protein kinase therapeutic strategies and involvement in Alzheimer's and various neurodegenerative abnormalities. *J Mol Neurosci* **43**, 376-390.
- [49] Han L, Yin K, Zhang S, Wu Z, Wang C, Zhang Q, Pan J, Chen B, Li J, Tan R, Xu Y (2013) Dalesconols B inhibits lipopolysaccharide induced inflammation and suppresses NF-kappaB and p38/JNK activation in microglial cells. *Neurochem Int* **62**, 913-921.
- [50] Bain J, McLauchlan H, Elliott M, Cohen P (2003) The specificities of protein kinase inhibitors: An update. *Biochem J* **371**, 199-204.
- [51] Lu Y, Zeff AS, Riegel AT (1993) Cloning and expression of a novel human DNA binding protein, PO-GA. *Biochem Biophys Res Commun* **193**, 779-786.
- [52] Thiele DJ (1992) Metal-regulated transcription in eukaryotes. *Nucleic Acids Res* **20**, 1183-1191.
- [53] Petronini PG, Alfieri R, Campanini C, Borghetti AF (1995) Effect of an alkaline shift on induction of the heat shock response in human fibroblasts. *J Cell Physiol* **162**, 322-329.
- [54] Costa RH, Grayson DR, Xanthopoulos KG, Darnell JE Jr (1988) A liver-specific DNA-binding protein recognizes multiple nucleotide sites in regulatory regions of transthyretin, alpha 1-antitrypsin, albumin, and simian virus 40 genes. *Proc Natl Acad Sci U S A* **85**, 3840-3844.
- [55] Scott GK, Daniel JC, Xiong X, Maki RA, Kabat D, Benz CC (1994) Binding of an ETS-related protein within the DNase I hypersensitive site of the HER2/neu promoter in human breast cancer cells. *J Biol Chem* **269**, 19848-19858.